Progress In Electromagnetics Research Letters, Vol. 39, 49–62, 2013

MINIATURIZED CROSSED-DIPOLE CIRCULARLY POLARIZED FRACTAL ANTENNA

Guo Liu*, Liang Xu, and Zhensen Wu

Institute of Radio Wave Propagation, Xidian University, Xi'an 710071, China

Abstract—A miniaturized crossed-dipole fractal antenna with circular polarization is presented in this letter. The radiating elements of the antenna were built as the Koch curve, and the antenna was mounted on a specially designed ground plane. The influence of ground plane to beamwidth and axial ratio of fractal antenna is also experimentally studied. The bandwidth of the VSWR $\leqslant 1.5:1$ within 3 dB axial ratio for the fractal antenna is about 5.98%. The measured results show that the proposed fractal antennas have good circular polarization property, efficiency and 23.4–33.5% size reduction comparing with the conventional crossed-dipole antenna. Furthermore, the comparison of the designed antenna and existing technique was also presented. The tested results are in good agreement with that of the simulations.

1. INTRODUCTION

Circularly polarized (CP) antennas can reduce the loss caused by the misalignment between the transmitter and receiver. They are useful in various modern wireless communications, such as satellite communication [1, 2], wireless local network (WLAN) [3], radio frequency identification (RFID) [4, 5], the global positioning system [GPS] [6, 7] and radar. Specially, crossed-dipole CP antennas are attractive among them because of their simple structure, low cost and ease of fabrication characteristics [8, 9]. Techniques for obtaining circular polarization with crossed dipole are classified into the radiating element and feed network types. The common practice is the use of power splitting and phasing networks [10, 11]. The technique presented in [12] established that it is possible to obtain circular polarization by

Received 5 February 2013, Accepted 29 March 2013, Scheduled 8 April 2013

* Corresponding author: Guo Liu (liuguosgg@hotmail.com).

proper choice of the dimensions of the radiating elements themselves. Those methods reported above are based on Euclidean geometry.

In this letter, a different technique is proposed to obtain a good circular polarization by using fractal concept. The term fractal, which means broken or irregular fragments, was originally coined by B. B. Mandelbrot [13] to describe a family of complex shapes, some of them having an inherent self-similarity in their geometrical structure. Combining aspects of the modern theory of fractal geometry with antenna design has received a lot of attention [14]. Fractals have been useful to design small, multiband, and high-directive antennas [15–20]. Koch curve is a good example of self-similar, space-filling fractals which have been used to develop wideband, multiband or miniaturized antennas [21–27]. The input resistance and reactance of the Koch monopoles can be effectively changed by changing number of iteration or the indentation angle [28]. So, circular polarization can be achieved by using two orthogonal fractal Koch dipoles with proper indentation angle and iterations, which ensures that the real part of their input admittances are equal and the phases of the input admittances differ by 90°. In practice, two kinds of fractal Koch crossed-dipole CP antennas excited by a hard coaxial cable with a slot were fabricated and successfully implemented.

2. DESIGN OF ANTENNAS

2.1. Construction of the Koch Curve

The standard Koch curve can be constructed iteratively replacing the central segment of the unit interval by two segments of length 1/3, both forming the upper part of an equilateral triangle [14]. The same procedure can be iterated an infinite number of times, each time replacing the central part of the remaining segments by a triangular cap, to obtain the ideal fractal Koch shape. When analyzing the fractal antenna behavior, it looked especially interesting to compare it with that of the closest Euclidean version, i.e., a straight monopole. Hereafter we name such a straight monopole as K_0 (the zero iteration of the fractal application), while the remaining objects of the iterations will be referred as K_1, K_2, ..., K_N, as shown in Fig. 1.

In the generalize Koch curve used here, the rotation (iteration) angle θ is variable. The common Koch curve is characterized by three factors: the iteration factor (IF), the iteration order (IO) and iteration angle (IA). The IF represents the construction law of fractal geometry generation, the IO depicts how many iteration processes are carried out and the IA confirms the angle of Koch curve of a particular iteration.

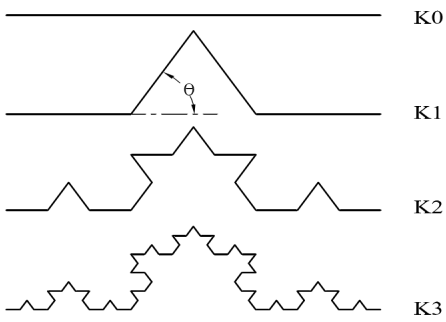

Figure 1. The iteration of the Koch curve.

As well known, the fractal dimension is considered an important mathematical property of fractals. Dimension of a fractal geometry can be defined in many ways, such as self-similarity dimension, topological dimension, Euclidean dimension and Hausdorff dimension. However, the most easily understood definition is self-similarity dimension. The fractal self-similarity dimension of the Koch curve can be varied by changing its indentation angle. In another word, the fractal dimension of the Koch curve is a function of θ, which is given by

$$D = \log N / \log s \tag{1}$$

where D = fractal dimension, s = scaling factor = $2(1 + \cos\theta)$, θ = indentation angle, and N = number of segments.

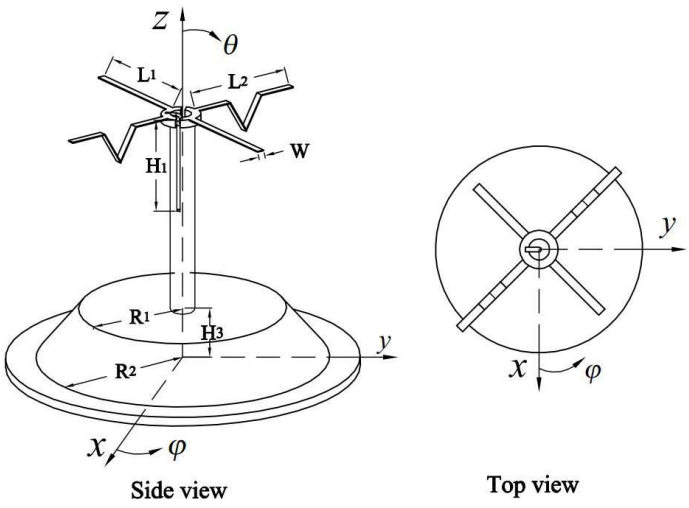

(a)

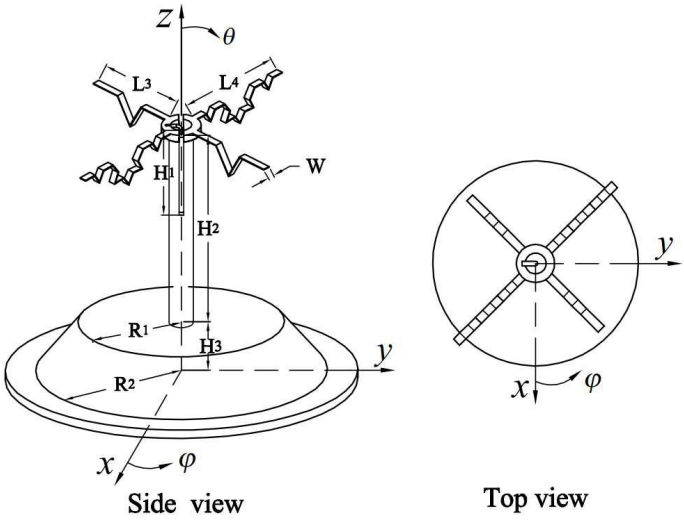

(b)

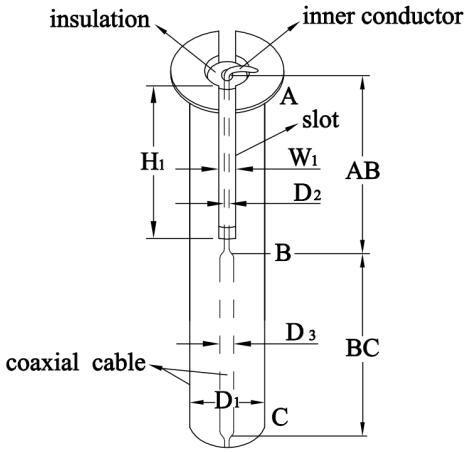

(c)

Figure 2. Geometry of the two CP fractal antennas. (a) Proposed antenna *a*. (b) Proposed antenna *b*. (c) Detail view of the feed structure.

2.2. Configurations and Analysis of Proposed Antenna

In this design, crossed-dipole CP antennas were fabricated on basis of Koch curve structure. Unlike the conventional crossed-dipole, the antenna radiation elements used here are not straight wires, they are

Koch curve. Two kinds of fractal Koch crossed-dipole CP antennas were fabricated in practice as shown in Fig. 2. Both antennas were designed for receiving with right-hand circular polarization (RHCP). The difference between them is the structure of the fractal dipoles. The two elements of crossed dipoles for antenna a follow the manner of K_0 and K_1 Koch curve, and antenna b with K_1 and K_2. It is known that the variation of fractal dimension is found to have a direct influence on the input impedance of Koch dipole antennas [28]. Circular polarization can be achieved by using the Koch curve elements with suitable iteration, which ensure that the real part of their input impedance is equal and the phases of the input admittances differ by 90°. In other words, the proper choose of indentation angle and lengths of the two elements L_1, L_2 and L_3, L_4 becomes the critical factor in producing the circular polarization wave. The length of individual dipole antennas was optimized to give the simulated input impedance and resultant phase

$$\text{Short elements } (L_1)\text{: } 51 - j53\,\Omega(-46^\circ)$$
$$\text{and Long elements } (L_2)\text{: } 49 + 47j(43^\circ)$$

Table 1. Simulated and measured results of the designed fractal antenna for different iterations.

Antenna	IO of two Koch dipole	IA of two Koch dipole	IF of two Koch dipole	Dimension	Bandwidth for 3 dB Axial ratio (%)		Bandwidth of VSWR ≤ 1.5 (%)	
					Simulated	Measured	Simulated	Measured
Antenna *a*	0, 1	0^o, 40^o	1, 0.33	1, 1.09	3.28	2.89	3.84	3.79
	0, 1	0^o, 50^o	1, 0.33	1, 1.16	4.65	4.23	5.96	5.78
	0, 1	0^o, 58^o	1, 0.33	1, 1.24	6.28	6.32	7.29	7.35
	0, 1	0^o, 60^o	1, 0.33	1, 1.26	6.96	6.86	7.54	7.71
	0, 1	0^o, 62^o	1, 0.33	1, 1.28	6.12	6.23	7.13	7.06
	0, 1	0^o, 70^o	1, 0.33	1, 1.41	4.35	4.23	5.26	5.14
Antenna *b*	1, 2	40^o, 40^o	0.33, 0.33	1.09, 1.09	4.86	4.23	3.28	3.16
	1, 2	50^o, 50^o	0.33, 0.33	1.16, 1.16	6.04	5.98	6.13	6.25
	1, 2	58^o, 58^o	0.33, 0.33	1.24, 1.24	6.74	6.62	7.02	7.78
	1, 2	60^o, 60^o	0.33, 0.33	1.26, 1.26	6.12	6.23	6.46	6.23
	1, 2	62^o, 62^o	0.33, 0.33	1.28, 1.28	5.49	5.31	5.89	5.92
	1, 2	70^o, 70^o	0.33, 0.33	1.41, 1.41	4.06	3.87	3.89	3.78

$$\text{Short elements } (L_3)\text{: } 48 - j46\,\Omega(-44^\circ)$$
$$\text{and Long elements } (L_4)\text{: } 51 + 50j(44^\circ)$$

It is clear that the relative phase difference between the two dipoles is close to 90°. Therefore, this design satisfies the phase requirement for CP propagation.

In order to achieve good axial ratio and bandwidth, optimization of indentation angle (IA), iteration factor (IF) and iteration order (IO) is done for the crossed-dipole CP antenna. Table 1 summarizes the simulated and measured results of the fractal CP antenna. It can be seen that good bandwidth and axial ratio is obtained when fractal dimension of Koch curve is (1, 1.26) for antenna a, and for antenna b it is (1.24, 1.24), IF = 0.33. Here as the number of iterations increases compactness of the design and the fabrication process becomes a bit different. So iteration order is limited to only two.

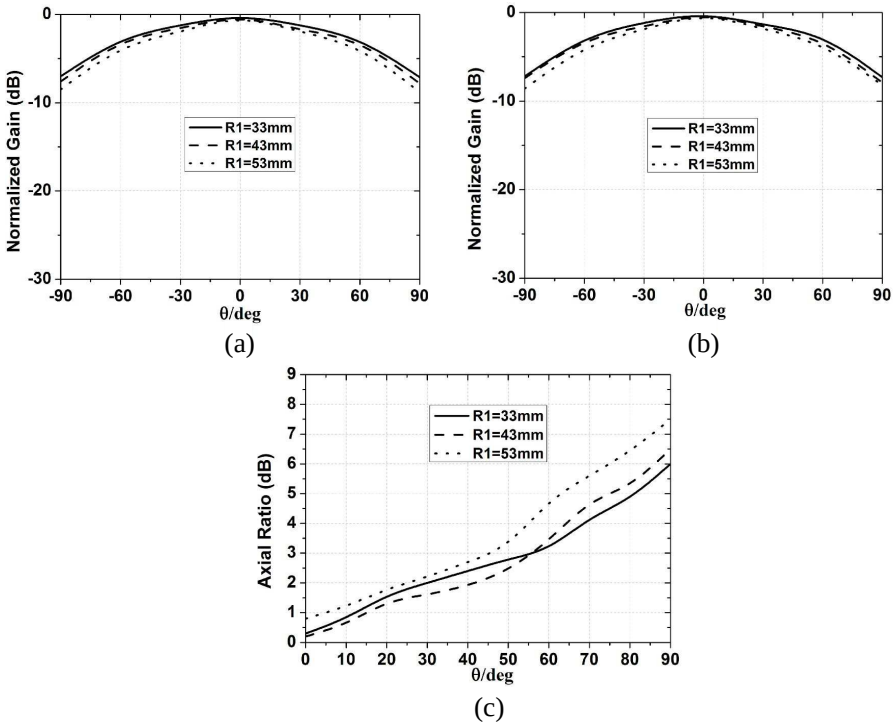

Figure 3. Measured radiation pattern cuts in (a) the x-z plane and (b) the y-z plane. (c) The effect of radius R_1 on the axial ratio of the antenna.

The antennas are excited by a customized hard coaxial cable with slot as shown in Fig. 2(c). The outer conductor was cut into two equal parts from the top, and it forms two slots. The inner conductor was connected to any part at the top. The width and length of the slot are W_1 and H_1. The diameters of the outside conductor is D_1 and the dielectric constant of insulation inside a coaxial cable is ε. The impedance of AB and BC segments are $Z_{\mathrm{AB}} = 50\,\Omega$, $Z_{\mathrm{BC}} = 25.5\,\Omega$ respectively. The input impedance of antenna Z_{A} is about $53\,\Omega$ at 2492 MHz. The slot works as a balun and $4:1$ impedance transformer. Therefore at the point B the impedance comes to $Z_{\mathrm{B}} = Z_{\mathrm{A}}/4 = 13\,\Omega$. In order to match Z_{B} to $50\,\Omega$ a $\lambda/4$ transmission line BC with $25.5\,\Omega$ impedance is designed, which means that: $Z_{\mathrm{BC}}^2/Z_{\mathrm{AB}} = (25.5 \times 25.5)/13 = 50\,\Omega$.

It is well known that the shape and size of the ground plane has big influence on antenna radiation characteristics. To achieve

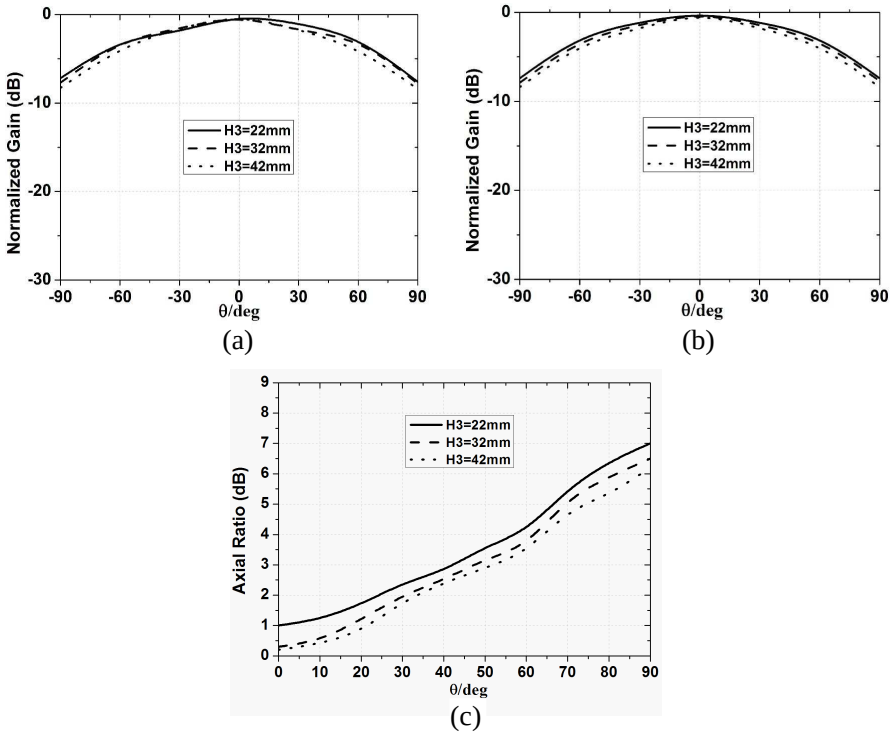

Figure 4. Measured radiation pattern cuts in (a) the x-z plane and (b) the y-z plane. (c) The effect of the height H_3 on the axial ratio of the antenna.

good radiation pattern, the proposed antennas were mounted on a specially designed ground plane. The lower radius R_2 was chosen to meet the profile restriction. The upper radius R_1 and the height H_3 were optimized for good axial ratio and beam width. The effects for various radiuses R_1 are given in Fig. 3 at 2492 MHz. It can be seen that the beamwidth becomes a bit narrow and the axial ratio of the antenna becomes worse at low angle if the radius R_1 increase. Fig. 4 shows the influence of the height H_3. The beamwidth is similar to each other in three cases, but the antenna axial ratio becomes worse if the height decrease as shown in Fig. 4(c). In the end a compromise choice are $R_1 = 43$ mm and $H_3 = 32$ mm. The proposed antennas have been simulated and optimized by using the software High Frequency Structure Simulator (HFSS). The final dimensions of the optimized antennas are: $L_1 = 24.9$ mm, $L_2 = 24.9$ mm, $L_3 = 21.6$ mm, $L_4 = 24.9$ mm, $H_1 = 20$ mm, $W_1 = 1$ mm, $D_1 = 5.2$ mm, $D_2 = 1$ mm, $D_3 = 1.8$ mm, $\varepsilon = 2.08$, $H_2 = 46$ mm, $H_3 = 32$ mm, $W = 1.1$ mm, $R_1 = 43$ mm, $R_2 = 78$ mm. The photographs of two practical CP fractal antennas are shown in Fig. 5.

Figure 5. Photographs of the two practical CP fractal antennas.

3. RESULTS AND DISCUSSIONS

The measurement is performed with Agilent 8753ES vector network analyzer and in Airlink 3D anechoic chamber. The simulated and measured VSWR of the proposed fractal CP antennas are presented in Fig. 6. It is observed that the measured results are in excellent agreement with simulation ones. The simulated impedance bandwidth (VSWR $\leqslant$ 1.5) of the antenna a is 7.54% (2408–2596 MHz) and the measured result is 7.71% (2395–2587 MHz), and for antenna b it is

7.02% (2445–2620 MHz), 7.78% (2416–2610 MHz) respectively. Fig. 7 shows the simulated and measured axial ratio (AR) versus frequency. For both antennas they all have good circular polarizations. The measured and simulated 3-dB AR bandwidth of antenna *a* is 6.86% (2368–2539 MHz) and 6.96% (2400–2579 MHz), and for antenna *b* it is about 6.62% (2400–2565 MHz), 6.74% (2392–2560 MHz) respectively. Specially, the measured bandwidths of the 1.5 VSWR within 3 dB AR of the antenna *a* and antenna *b* are about 5.78% (2395–2539 MHz) and 5.98% (2416–2565 MHz), meanwhile for conventional antenna it is 5.86% (2412–2558 MHz). These results show that the proposed CP fractal antennas obtain similar bandwidths and even it is a bit wider for the antenna *b*.

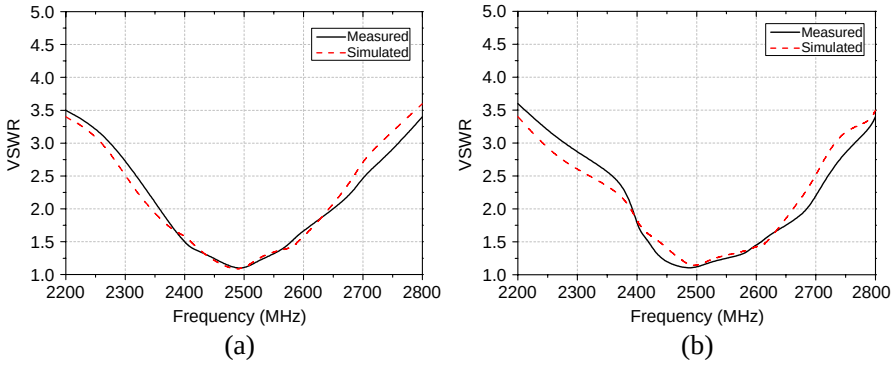

Figure 6. Measured and simulated VSWR for the designed CP fractal antennas. (a) Proposed antenna *a*. (b) Proposed antenna *b*.

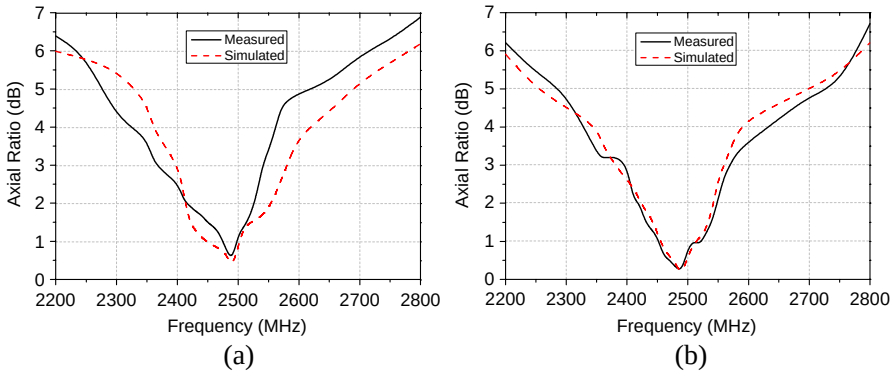

Figure 7. Measured and simulated AR for the designed CP fractal antennas. (a) Proposed antenna *a*. (b) Proposed antenna *b*.

The measured radiation patterns and gains for the two fractal antennas and normal crossed-dipole antenna on the center frequency 2492 MHz are given in Fig. 8. It is shown that they are similar to each other, which means that the fractal Koch structure does not have obvious influence on antenna efficiency although the antenna size is significantly reduced. But it is noticed that the un-roundness patterns at low angle ($\theta = 70°$) of fractal antennas are a bit better

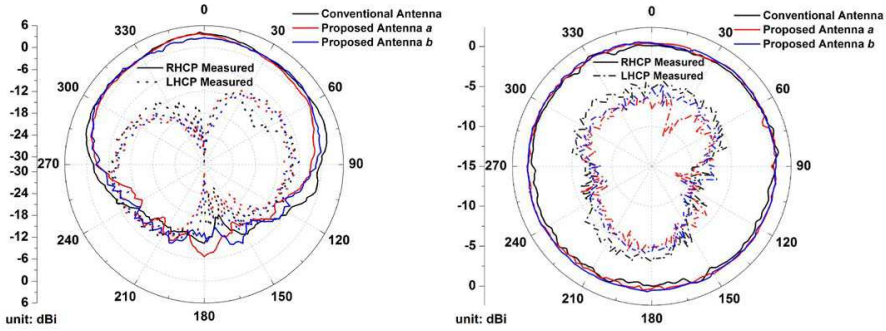

Figure 8. The measured radiation patterns at 2492 MHz. (a) y-z plane. (b) x-y plane at $\theta = 70°$.

Table 2. Performance comparisons between the proposed antennas and conventional crossed dipole antenna.

Antenna	Conventional Antenna	Antenna a	Antenna b
Dipole structure	K_0, K_0	K_0, K_1	K_1, K_2
Fractal dimension	1, 1	1, 1.26	1.24, 1.24
Length of dipoles (mm)	24.9, 32.5	24.9, 24.9	21.6, 24.9
Centre Frequency (MHz)	2492	2492	2492
3 dB Axial ratio bandwidth (%)	6.25	6.86	6.62
Bandwidth of VSWR$\leq$ 1.5 (%)	7.84	7.71	7.78
Bandwidth of 3 dB AR with VSWR $\leq$ 1.5 (%)	5.86	5.78	5.98
Gain in the main direction (dBi)	3.4	3.1	2.9

Table 3. Performance comparisons between the proposed antennas and other CP antenna (as introduced in [4]).

Antenna	Antenna *a*	Antenna *b*	RFID Antenna in [4]
Type of dipole structure	Koch	Koch	Meander-line
Centre Frequency (MHz)	2492	2492	925
3 dB axial ratio bandwidth (%)	6.86	6.62	3.3
3-dB axial ratio beamwidth	128°	132°	80°
Bandwidth of VSWR $\leq$ 2 (%)	11.9	11.7	11.8
Measured peak gain (dBi)	3.1	2.9	1.4
Commercial application	Vehicle satellite navigation system	Vehicle satellite navigation system	RFID handheld reader

than that of conventional antenna (as shown in Fig. 8(b)). It can be explained like that the Koch elements have changed the current distributions along with the radiating arms, and this improved the low-angle radiation. In addition, the comparisons for the tested results are listed in Table 2. It can be seen that the sizes of the two Koch fractal antennas are reduced by 23.4%, 33.5% respectively comparing with that of the conventional crossed-dipole antenna. In other words, the proposed antennas can operate at lower frequency with the same size. Furthermore, the comparison of the designed antenna and existing solutions (as introduced in [4]) was presented in Table 3. It is clear that the proposed CP antenna has wider 3 dB AR bandwidth and beamwidth. This individual characteristic made it very useful for vehicle satellite navigation system.

4. CONCLUSION

In this paper, two fractal Koch crossed-dipole CP antennas have been proposed and successfully implemented. The measured results show that it is possible to obtain circular polarization by proper

choice of the Koch element. Furthermore, the relationship between fractal dimension and bandwidth, axial ratio of fractal CP antenna is experimentally studied. The proposed fractal CP antennas have good circular polarization property, radiation patterns, efficiency and 23.4–33.5% size reduction. This miniaturized wide-beam CP antenna is very useful for vehicle Beidou satellite navigation receiver system at S-band.

ACKNOWLEDGMENT

The authors would like to thank the Fundamental Research Funds for the Central Universities and the National Natural Science Foundation of China under Grant No. 61179021 to support this kind of research.

REFERENCES

1. Exposito-Dominguez, G., J.-M. Fernandez Gonzalez, P. Padilla de la Torre, and M. Sierra-Castaner, "Dual circular polarized steering antenna for satellite communications in X band," *Progress In Electromagnetics Research*, Vol. 122, 61–76, 2012.
2. Trinh-Van, S., H. B. Kim, G. Kwon, and K. C. Hwang, "Circularly polarized spidron fractal slot antenna arrays for broadband satellite communications in Ku-band," *Progress In Electromagnetics Research*, Vol. 137, 203–218, 2013.
3. Khidre, A., K. F. Lee, F. Yang, and A. Elsherbeni, "Wideband circularly polarized E-shaped patch antenna for wireless applications," *IEEE Antennas and Propagation Magazine*, Vol. 52, No. 5, 219–229, Oct. 2010.
4. Lin, Y.-F., Y.-K. Wang, H.-M. Chen, and Z.-Z. Yang, "Circularly polarized crossed dipole antenna with phase delay lines for RFID handheld reader," *IEEE Trans. Antennas Propag.*, Vol. 60, No. 3, 1221–1227, Mar. 2012.
5. Wang, P., G. Wen, J. Li, Y. Huang, L. Yang, and Q. Zhang, "Wideband circularly polarized UHF RFID reader antenna with high gain and wide axial ratio beamwidths," *Progress In Electromagnetics Research*, Vol. 129, 365–385, 2012.
6. Heidari, A. A., M. Heyrani, and M. Nakhkash, "A dual-band circularly polarized stub loaded microstrip patch antenna for GPS applications," *Progress In Electromagnetics Research*, Vol. 92, 195–208, 2009.
7. Bao, X. L., G. Ruvio, M. J. Ammann, and M. John, "A novel GPS patch antenna on a fractal Hi-impedance surface substrate,"

IEEE Antennas Wireless Propaga. Lett., Vol. 5, No. 1, 323–326, Dec. 2006.

8. Jibrael, F. J., "Multiband cross dipole antenna based on the triangular and quadratic fractal Koch curve," *International Journal of Engineering*, Vol. 4, No. 3, 2010.
9. Jibrael, F. J., W. S. Mummo, and M. T. Yaseen, "Multiband cross fractal dipole antenna for UHF and SHF applications," *2010 IEEE Int. Conf. on Wireless Communications, Networking and Information Security*, 219–223, Jun. 2010.
10. Cebik, L. B., "The turnstile antenna. An omni-directional horizontally polarized antenna," http://www.cebik.com/turns.html.
11. Qiu, J., B. Zhao, and L. Zhong, "A kind of new minimize technology of circular polarization antenna," *International Conference on Microwave and Millimeter Wave Technology*, 1–3, Apr. 2007.
12. Bolster, M. F., "A new type of circular polarizer using crossed dipoles," *IRE Trans. on Microwave Theory and Techniques*, Vol. 9, No. 5, 385–388, Sep. 1961.
13. Mandelbrot, B. B., *The Fractal Geometry of Nature,* Freeman, New York, 1983.
14. Puente, C., J. Romeu, and A. Cardama, "Fractal-shaped antennas," *Frontiers in Electromagnetics*, 48–93, D. H. Werner and R. Mittra, Eds., 1999.
15. Gianvittorio, J. P. and Y. Rahmat-Samii, "Fractal antennas: A novel antenna miniaturization technique, and application," *IEEE Antennas and Propagation Magazine*, Vol. 44, No. 1, 20–36, Feb. 2002.
16. Anguera, J., E. Martinez, C. Puente, C. Borja, and J. Soler, "Broad-band triple-frequency microstrip patch radiator combing a dual-band modified Sierpinski fractal and a monoband antenna," *IEEE Trans. Antennas Propag.*, Vol. 54, No. 11, 3367–3373, Nov. 2006.
17. Anguera, J., C. Puente, C. Borja, and J. Soler, "Fractal-shaped antenna: A review," *Wiley Encyclopedia of RF and Microwave Engineering*, Vol. 2, 1620–1635, 2005.
18. Song, C. T. P., P. S. Hall, H. Ghafouri-Shiraz, and D. Wake, "Sierpinski monopole antenna with controlled band spacing and input impedance," *IEE Electronic Letters*, Vol. 35, No. 13, 1036–1037, Jun. 1999.
19. Anguera, J., J. P. Daniel, C. Borja, J. Mumbrú, C. Puente, T. Leduc, N. Laeveren, and P. Van Roy, "Metallized foams

for fractal-shaped microstrip antennas," *IEEE Antennas and Propagation Magazine*, Vol. 50, No. 6, 20–38, Dec. 2008.

20. Li, D. and J. Mao, "Koch-like sided Sierpinski Gasket multifractal dipole antenna," *Progress In Electromagnetics Research*, Vol. 126, 399–427, 2012.
21. Baliarda, C. P., J. Romeu, and A. Cardama, "The Koch monopole: A small fractal antenna," *IEEE Trans. Antennas Propag.*, Vol. 48, No. 11, 1773–1781, Nov. 2000.
22. Yu, Z.-W., G.-M. Wang, X.-J. Gao, and K. Lu, "A novel small-size single patch microstrip antenna based on koch and sierpinski fractal-shapes," *Progress In Electromagnetics Research Letters*, Vol. 17, 95–103, 2010.
23. Karim, M. N. A., M. K. Abd Rahim, H. A. Majid, O. B. Ayop, M. Abu, and F. Zubir, "Log periodic fractal Koch antenna for UHF band applications," *Progress In Electromagnetics Research*, Vol. 100, 201–218, 2010.
24. Chen, W. L., G. M. Wang, and C. X. Zhang, "Small-size microstrip patch antennas combining Koch and Sierpinski fractal-shapes," *IEEE Antennas Wireless Propaga. Lett.*, Vol. 7, 738–741, 2008.
25. Kordzadeh, A. and F. Hojjat-Kashani, "A new reduced size microstrip patch antenna with fractal shaped defects," *Progress In Electromagnetics Research B*, Vol. 11, 29–37, 2009.
26. Lin, S., X. Liu, and X.-R. Ma, "Design and analysis of a novel CPW-FED Koch fractal Yagi-Uda antenna with small electric length," *Progress In Electromagnetics Research C*, Vol. 33, 67–79, 2012.
27. Li, D. and J.-F. Mao, "Sierpinskized Koch-like sided multifractal dipole antenna," *Progress In Electromagnetics Research*, Vol. 130, 207–224, 2012.
28. Vinoy, K. J., J. K. Abraham, and V. K. Varadan, "On the relationship between fractal dimension and the performance of multi-resonant dipole antennas using Koch curves," *IEEE Trans. Antennas Propag.*, Vol. 51, No. 9, 2296–2303, Sep. 2003.